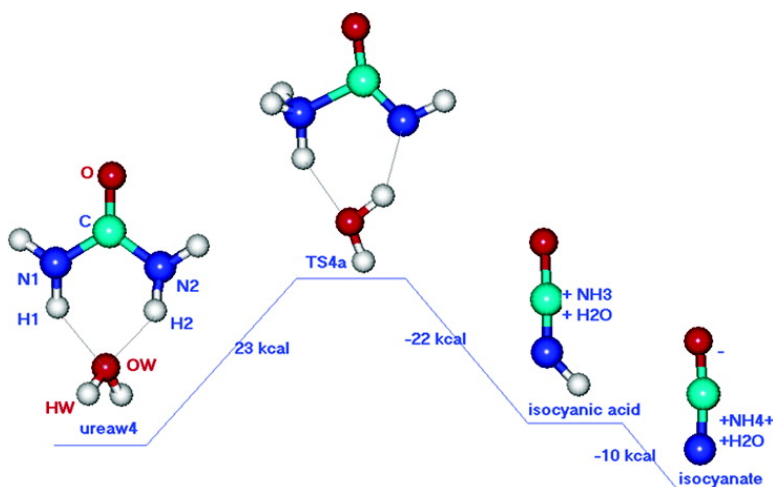


The Hydrolysis of Urea and the Proficiency of Urease

Guillermina Estiu, and Kenneth M. Merz

J. Am. Chem. Soc., **2004**, 126 (22), 6932-6944 • DOI: 10.1021/ja049327g • Publication Date (Web): 07 May 2004

Downloaded from <http://pubs.acs.org> on March 31, 2009



More About This Article

Additional resources and features associated with this article are available within the HTML version:

- Supporting Information
- Links to the 6 articles that cite this article, as of the time of this article download
- Access to high resolution figures
- Links to articles and content related to this article
- Copyright permission to reproduce figures and/or text from this article

[View the Full Text HTML](#)

The Hydrolysis of Urea and the Proficiency of Urease

Guillermina Estiu and Kenneth M. Merz, Jr.*

Contribution from the Department of Chemistry, The Pennsylvania State University,
152 Davey Laboratory, University Park, Pennsylvania 16802-6300

Received February 6, 2004; E-mail: merz@psu.edu

Abstract: We present the results of a computational study of the solution phase decomposition of urea, which provides insight into probable reaction pathways for the urease-catalyzed reaction. Calculations, which were used to derive thermodynamic parameters that were further used for a kinetic analysis, have been done at the solvent-corrected MP2/6-311++G** level. Both elimination and hydrolytic pathways have been considered. Elimination is favored for the solution phase reaction, which proceeds by H-bond coordination of a water molecule to the amine nitrogen atoms. The coordination of one water molecule greatly facilitates the reaction by allowing it to proceed through a cyclic six-member transition state. Aspects of the water-urea H-bond interactions have also provided insights into critical aspects of the hydrogen bond pattern in the urease active site. On the basis of a kinetic analysis, we have estimated the proficiency of urease and have predicted that it is the most proficient enzyme identified to date.

1. Introduction

Urea is one of the simplest known biologically relevant molecules. Significant research effort has dealt with understanding urea reactivity in both catalytic and noncatalytic media.^{1–11} Nonetheless, there still is uncertainty regarding the interpretation and nature of the aqueous phase reactivity of urea, for which unimolecular elimination and bimolecular elimination/hydrolysis mechanisms have been described.^{8,9} Moreover, urea is unusually stable because of its resonance stabilization (estimated to be 30–40 kcal/mol),¹² which decreases the electrophilicity of the carbonyl carbon. These mechanisms are related, respectively, to intramolecular and intermolecular proton-transfer reactions involving both amino groups or the amino and the carbonyl groups. The intermolecular mechanism proceeds with the assistance of a water molecule and can follow elimination or hydrolytic pathways. The catalytic decomposition of urea is accomplished by the well-characterized enzyme urease. It is thought that the enzyme mechanism is a hydrolysis reaction rather than the elimination reaction.

Enzyme proficiency is used to quantify the catalytic power of a given enzyme for a specific reaction type. It indicates how

tightly the ligand is bound to the substrate in the transition state and is measured by $(k_{\text{cat}}/K_{\text{m}})/k_{\text{non}}$.^{13,14} It has been successfully determined in several cases, giving values that range between 10^8 and 10^{23} M^{-1} . The highest value has been determined for OMP decarboxylase, a key enzyme in the biosynthesis of nucleic acids, effecting the decarboxylation of oritidine 5'-monophosphate to form uridine 5'-monophosphate.^{13–16} However, the determination of the proficiency requires the same mechanisms to occur in the catalyzed and the uncatalyzed reactions. In cases where the enzyme-catalyzed reaction and the solution phase reaction differ, this determination is hampered, because k_{non} cannot be obtained experimentally. The enzyme urease offers just such a situation. The enzyme is thought to catalyze urea hydrolysis to ammonia and carbon dioxide,^{1–4} while the low energy solution phase pathway is an elimination reaction that leads to the ammonium ion and cyanate. The uncatalyzed hydrolysis of urea has not been observed experimentally and is presumed to be higher in energy than the elimination reaction. The enzymatic hydrolysis of urea has biologically important consequences. In addition to decreasing the efficiency of urea as a soil fertilizer, urease activity is known to be involved in human and animal infections of the urinary and gastrointestinal tracts.^{5–7}

Understanding the factors that define the preference for either the hydrolytic or the elimination pathways, as a function of the experimental conditions (i.e., catalyzed versus uncatalyzed, respectively), will increase our understanding of how urease overcomes the resonance stabilization of urea and favors the less favorable hydrolytic decomposition. The $k_{\text{cat}}/K_{\text{m}}$ of urease is 10^{14} -fold higher than the rate of the uncatalyzed elimination reaction, implying that the proficiency of urease is $>10^{14}$, because the uncatalyzed hydrolysis reaction must be even slower.¹

- (1) Karplus, P. A.; Pearson, M. A.; Hausinger, R. P. *Acc. Chem. Res.* **1997**, *30*, 330.
- (2) Todd, M. J.; Hausinger, R. P. *Biochemistry* **2000**, *39*, 5389.
- (3) Pearson, M. A.; Schaller, R. A.; Michel, L. O.; Karplus, P. A.; Hausinger, R. P. *Biochemistry* **1998**, *37*, 6214.
- (4) Jabri, E.; Karplus, P. A. *Biochemistry* **1996**, *35*, 10616.
- (5) Mobley, H. L.; Island, M. D.; Hausinger, R. P. *Microbiol. Rev.* **1995**, *59*, 451.
- (6) Covacci, A.; Telford, J. L.; Del Giudice, G.; Parsonnet, J.; Rappuoli, R. *Science* **1999**, *284*, 1328.
- (7) Ha, N.-C.; Oh, S.-T.; Sung, J. Y.; Cha, K. A.; Lee, M. H.; Oh, B.-H. *Nat. Struct. Biol.* **2001**, *8*, 505.
- (8) Shaw, H. R.; Walker, D. G. *J. Am. Chem. Soc.* **1958**, *80*, 5337 and references therein.
- (9) Laidler, K. J.; Hoare, J. P. *J. Am. Chem. Soc.* **1950**, *72*, 2489.
- (10) Dixon, N. E.; Gazzola, C.; Blakeley, R. L.; Zerner, B. *J. Am. Chem. Soc.* **1975**, *97*, 4131.
- (11) Zerner, B. *Bioorg. Chem.* **1991**, *19*, 116.
- (12) Wheland, G. W. *Resonance in Organic Chemistry*; Wiley: New York, 1955.

- (13) Wolfenden, R.; Snider, M. J. *Acc. Chem. Res.* **2001**, *34*, 938.
- (14) Radzicka, A.; Wolfenden, R. *Science* **1995**, *267*, 90.
- (15) Warshel, A.; Strajbl, M.; Villa, J.; Florian, J. *Biochemistry* **2000**, *29*, 14728.
- (16) Phillips, L. M.; Lee, J. K. *J. Am. Chem. Soc.* **2001**, *123*, 12067.

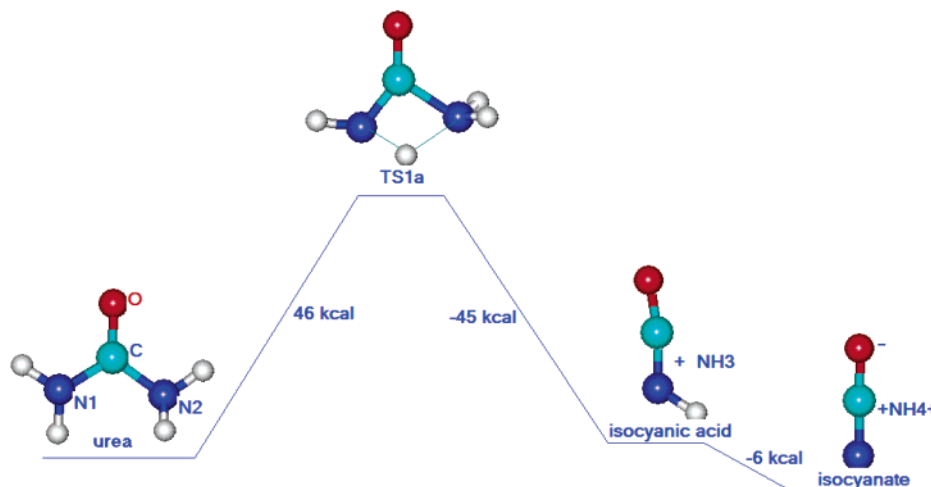


Figure 1. Reaction profile for urea elimination decomposition pathway leading to isocyanic acid. The structures correspond to stationary points on the potential hyper surface. ΔG_{act} values, calculated at the MP2/6-311++G** level, are solvent-corrected. Relative energies are not drawn to scale.

On the basis of the uncertainty regarding the mechanistic details of the elimination and hydrolysis decomposition of urea, we decided to perform a thorough study of the solution phase decomposition of urea, focusing on the evaluation of the associated rate constants, which would then allow an estimation of urease proficiency. We have applied high-level quantum chemical calculations to analyze different urea decomposition pathways to choose the one most likely to match the enzymatic one. We provide a general scheme that leads to conclusions that are in agreement with and extend the available experimental observations. Moreover, we are able to provide further insight into the proficiency of the catalytic mechanism of urease. The kinetic study offers, on the other hand, valuable information that characterizes the mechanisms of classic reactions involving small molecules of interest in organic synthesis. This is not only the case of urea itself,¹⁷ but also of cyanamide and cyanic acid, which have been extensively analyzed recently.^{18,19} These small molecules are related to urea, and their reactivity share several common patterns with it.

2. Computational Methods

All the calculations have been performed at the MP2/6-311++G** level of theory, using the Gaussian 98 suite of programs.²⁰ Structural parameters and associated energies for reactants, products, stable intermediates, and transition states result from full geometry optimization procedures, with no imposed constraints. Search for stationary points of the potential energy surface followed gradient-based algorithms and quadratic synchronous transit (QST2) approaches. Critical points have been further characterized by analytical computation of the vibrational frequencies at the same level of theory. Bulk solvent effects (water) are described via an isodensity continuum polarizable

model.²¹ Atomic charges were computed according to the Merz–Kollman approximation,²² again at the same level of theory.

The thermodynamic functions (free energy G , entropy S , enthalpy H) have been calculated using MP2/6-311++G** frequencies. Values for different temperatures, ranging between 298.15 and 373.15 K, were obtained from the contributions of translational, rotational, and vibrational partition functions. Using these calculated values, we evaluated the activation energies from Eyring plots of $\ln k$ vs $1/T$.

3. Results

The potential energy surfaces for several different reaction mechanisms were investigated. The first set of mechanisms examined (Figures 1 and 2) were the unimolecular elimination reactions involving different intermediate types. For the reactions assisted by either one or two water molecules, both the elimination and hydrolytic pathways have been considered (Figures 3, 4, 6, and 7).

Our interest focused on the study of the solution phase hydrolysis of urea, which would also provide the necessary data to further calculate the proficiency of urease. To gain confidence in the accuracy of the calculated kinetic parameters, we analyzed in detail the elimination mechanism for which experimental data were available.^{8,9} We compared different possible pathways until we were able to propose reaction mechanisms with associated rate constants and activation energies in agreement with experiment. We provide in the following a thorough discussion of the elimination and hydrolytic pathways for the uncatalyzed decomposition of urea.

3.1. The Elimination Pathway for Urea Decomposition.

Experimental and theoretical data have shown that the most stable conformer of urea exhibits an anti-conformation of C_2 symmetry with the H atoms of the NH_2 groups pyramidalized and pointing in opposite directions relative to the plane defined by the heavy atoms of the molecule.^{23–26} Urea can also exist in a syn-conformation of C_s symmetry, with the H atoms of the

- (17) Tshipis, C. A.; Karidipis, P. A. *J. Am. Chem. Soc.* **2003**, *121*, 12067.
 (18) Gardebien, F.; Sevin, A. *J. Phys. Chem. A* **2003**, *107*, 3925.
 (19) Tordini, F.; Bencini, A.; Bruschi, M.; De Gioia, L.; Zampella, G.; Fantucci, P. *J. Phys. Chem. A* **2003**, *107*, 1188.
 (20) Frisch, M. J.; Trucks, G. W.; Schlegel, H. B.; Scuseria, G. E.; Robb, M. A.; Cheeseman, J. R.; Zakrzewski, V. G.; Montgomery, J. A., Jr.; Stratmann, R. E.; Burant, J. C.; Dapprich, S.; Millam, J. M.; Daniels, A. D.; Kudin, K. N.; Strain, M. C.; Farkas, O.; Tomasi, J.; Barone, V.; Cossi, M.; Cammi, R.; Mennucci, B.; Pomelli, C.; Adamo, C.; Clifford, S.; Ochterski, J.; Petersson, G. A.; Ayala, P. Y.; Cui, Q.; Morokuma, K.; Malick, D. K.; Rabuck, A. D.; Raghavachari, K.; Foresman, J. B.; Cioslowski, J.; Ortiz, J. V.; Stefanov, B. B.; Liu, G.; Liashenko, A.; Piskorz, P.; Komaromi, I.; Gomperts, R.; Martin, R. L.; Fox, D. J.; Keith, T.; Al-Laham, M. A.; Peng, C. Y.; Nanayakkara, A.; Gonzalez, C.; Challacombe, M.; Gill, P. M. W.; Johnson, B. G.; Chen, W.; Wong, M. W.; Andres, J. L.; Head-Gordon, M.; Replogle, E. S.; Pople, J. A. *Gaussian 98*, revision A.6; Gaussian, Inc.: Pittsburgh, PA, 1998.

- (21) Foresman, J. B.; Keith, T. A.; Wiberg, K. B.; Snoonian, J.; Frisch, M. J. *J. Phys. Chem.* **1996**, *100*, 16098.
 (22) Besler, B. H.; Merz, K. M.; Kollman, P. A. *J. Comput. Chem.* **1990**, *11*, 431.
 (23) Rousseau, B.; Van Alsenoy, C.; Keuleers, R.; Desseyn, H. O. *J. Phys. Chem. A* **1998**, *102*, 6540.
 (24) King, S. T. *Spectrochim. Acta, Part A* **1972**, *28*, 165.
 (25) Brown, R. D.; Godfrey, P. D.; Stoney, J. J. *Mol. Spectrosc.* **1975**, *58*, 445.
 (26) Li, X.; Stotesbury, S. J.; Jayasooriya, U. A. *Spectrochim. Acta, Part A* **1987**, *43*, 1595.

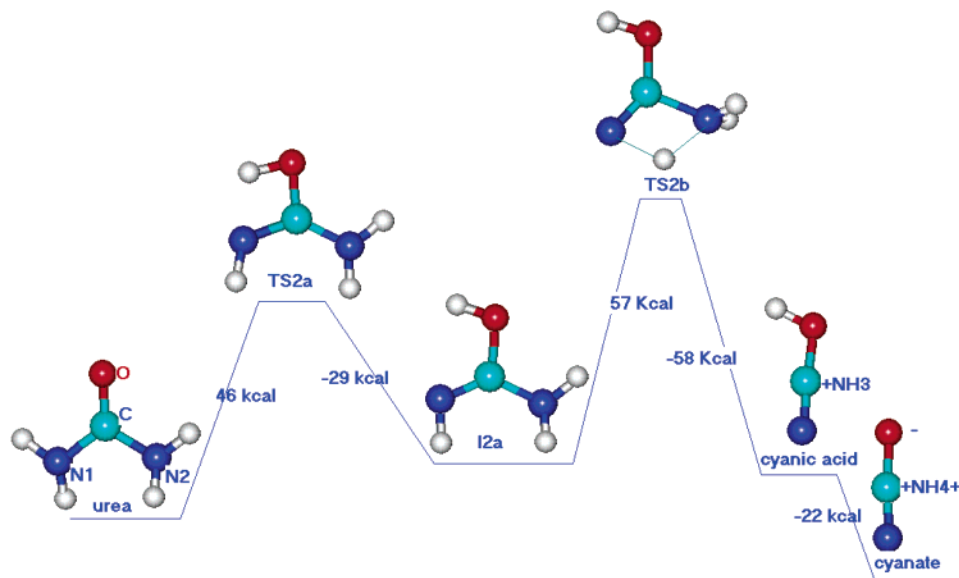


Figure 2. Reaction profile for urea decomposition involving urea isomerization leading to cyanic acid. The structures correspond to stationary points in the potential hyper surface. ΔG_{act} values, calculated at the MP2/6-311++G** level, are solvent-corrected. Relative energies are not drawn to scale.

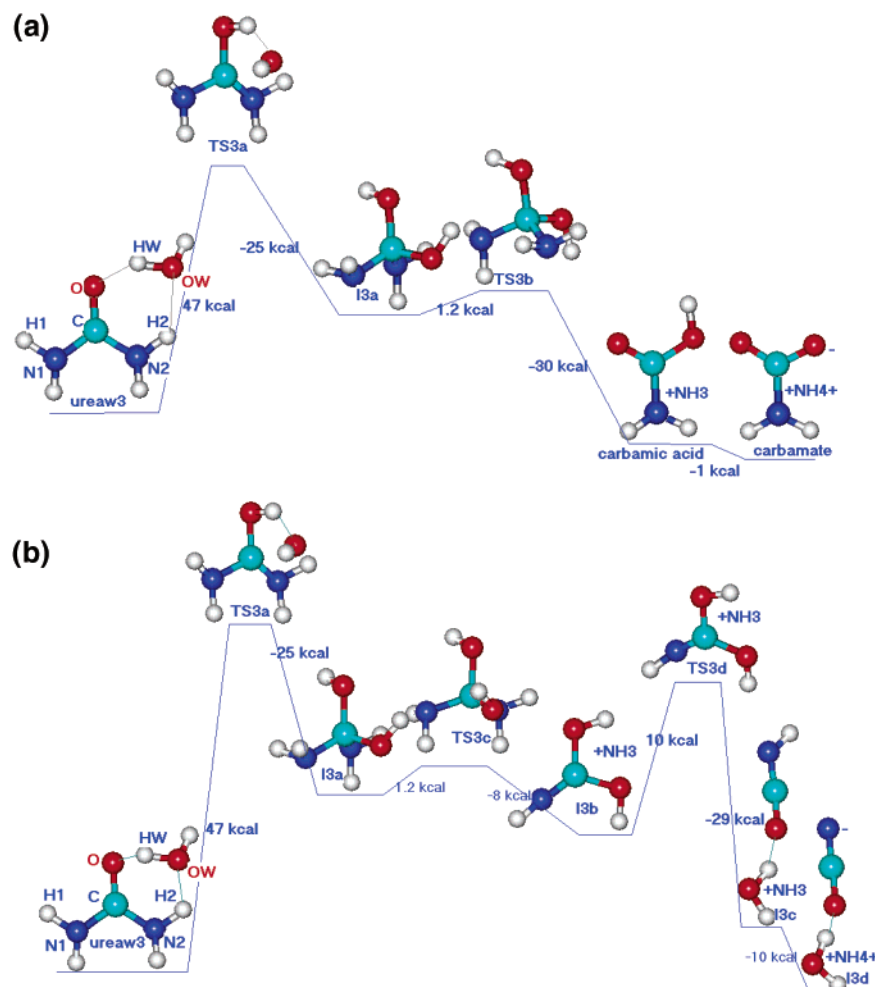


Figure 3. (a) Reaction profile for the urea hydrolytic pathway assisted by one water molecule, leading to carbamic acid. (b) Reaction profile for the urea elimination pathway assisted by one water molecule, leading to cyanic acid. The structures correspond to stationary points in the potential hyper surface. ΔG_{act} values, calculated at the MP2/6-311++G** level, are solvent-corrected. Relative energies are not drawn to scale.

NH_2 groups pyramidalized to the same side. We calculate the latter to be 1.2 kcal/mol less stable than the C_2 isomer, at the MP2/6-311++G** level. The structural parameters derived

from our calculations are reported in Table 1. Experimental data are also provided, together with results of calculations performed at different levels of theory.

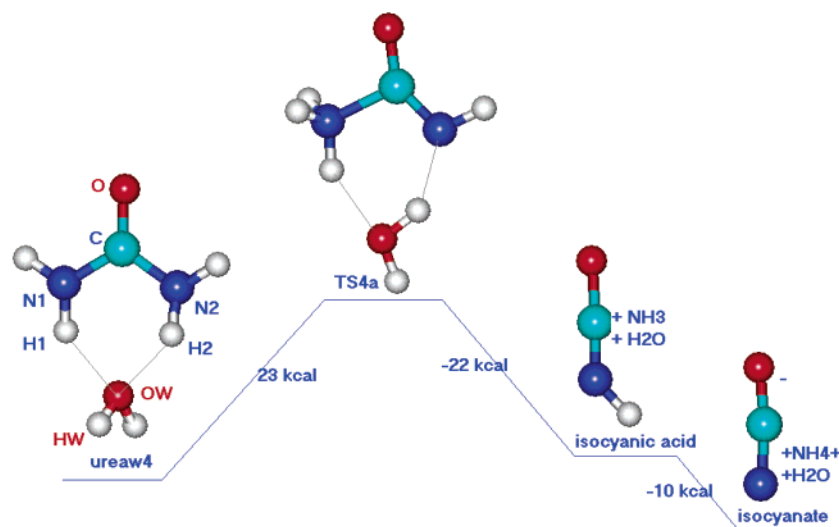


Figure 4. Reaction profile for the urea elimination pathway assisted by one water molecule, leading to isocyanic acid. G_{act} values, calculated at the MP2/6-311++G** level, are solvent corrected. Relative energies are not drawn to scale.

Table 1. Relevant Structural Parameters (Interatomic Distances in Å, Angles in Degrees)^a

	r_{CO}	r_{CN1}	r_{CN2}	r_{NH1}	r_{NH2}	$\angle\text{NHN}$
urea ^b	1.218	1.391	1.391	1.010	1.010	113.1
urea ^c	1.221	1.378	1.378	1.021	1.021	
urea ^d	1.229	1.388	1.388			112.5
urea ^e	1.226	1.338	1.338			114.2
urea ^f	1.221	1.389	1.389	1.010	1.010	113.6
TS1a	1.209	1.332	1.576	1.338	1.256	111.6
isocyanic acid	1.173	1.225		1.008		
isocyanate	1.188	1.209				

^a Calculated at the MP2/6-311++G** level for the elimination reaction pathway shown in Figure 1. ^b This work. ^c Experimental (microwave) data, ref 23. ^d MP2/6-31+G*, ref 27. ^e B3LYP/6-31+G*, ref 27. ^f B3LYP/6-31G**, ref 17.

The elimination mechanism for urea decomposition was proposed in the early 1950s and has been widely accepted since that time. The reaction proceeds through a planar four-center transition state that involves intramolecular proton transfer between the amino groups. This pathway generates the experimentally observed products (isocyanic acid and ammonia) with a calculated free energy of activation (ΔG_{act}) of 47 kcal/mol (Figure 1). The calculated value is largely unaffected by the inclusion of solvent (water) via a continuum approach. Solvent modeling only decreases the computed activation free energy by 1 kcal/mol. Nevertheless, the solvent strongly stabilizes the products as charged species (Table 2). The reaction would not be possible in the absence of solvent, because the neutral products, which are more stable than the charged ones in a vacuum, have higher energy than the reactants. Relevant

characteristics of the products, reactants transition states (TS), and intermediates are summarized in Table 1.

A similar TS has been recently proposed in a theoretical study of the Wohler synthesis of urea.¹⁷ The calculations, performed at the B3LYP/6-31G** level, identified this TS in a mechanistic study of the addition of ammonia to the CN double bond of isocyanic acid. Despite being structurally similar to ours, the reported energy difference between urea and the TS is 10 kcal/mol higher. This difference cannot be easily explained, because B3LYP tends to slightly underestimate the energy barriers in proton-transfer reactions.²⁷ Even though solvent effects were not previously examined, we do not assign the energy difference to solvation. Our own results show no solvent dependence on the activation energy. Nevertheless, we do predict a significant influence of the solvent on the exothermicity calculated for the Wohler synthesis, because the stability of ammonia and isocyanic acid are strongly dependent on solvation.

The second unimolecular elimination mechanism has a related intramolecular proton transfer, but this time it involves the amino groups of the enol tautomer of urea. The associated free energy arises from two contributions. The first is the energy required for the keto–enol tautomerization, while the second involves the interamino proton-transfer step. (Figure 2 and Table 3). The calculated ΔG_{act} is 74 kcal/mol, which is much higher (by 27 kcal/mol) than the previous reaction (Figure 1). This mechanism involves two planar four-center transition states. The first one is associated with the transformation of urea to isourea (TS_{2a}). The second one (TS_{2b}) is similar to the one shown in Figure 1, but via isourea (I_{2a}) rather than urea. The barrier height is defined

Table 2. Electronic (E, au) and Free Energies (G, au, 298 K, 1 bar) Derived from Gas Phase and ICPM (Solvent = Water) Calculations^a

	E gas phase (au)	E solvent	G gas phase (au)	G solvent (au)
urea	-224.756496	-224.772684	-224.718067	-224.734255
TS1a	-224.676397	-224.690812	-224.644110	-224.660953
isocyanic acid	-168.311859	-168.318144	-168.323607	-168.329892
NH ₃	-56.415524	-56.422829	-56.399747	-56.403053
isocyanic acid + NH ₃	-224.727383	-224.740973	-224.723354	-224.732944
isocyanate	-167.757603	-167.860627	-167.779818	-167.882842
NH ₄ ⁺	-56.755685	-56.889853	-56.725201	-56.859367
isocyanate + NH ₄ ⁺	-224.513288	-224.750478	-224.505019	-224.742209

^a (MP2/6-311++G** level of theory) for the species involved in the different steps of the reaction shown in Figure 1.

Table 3. Electronic (E, au) and Free Energies (G, au, 298 K, 1 bar) Derived from Gas Phase and ICPM (Solvent = Water) Calculations^a

	E gas phase (au)	E solvent (au)	G gas phase (au)	G solvent (au)
urea	-224.756496	-224.772684	-224.718067	-224.734255
TS2a	-224.679462	-224.693416	-224.646580	-224.660534
I2a	-224.727463	-224.744058	-224.690192	-224.706787
TS2b	-224.625100	-224.646894	-224.589929	-224.615323
cyanic acid	-168.273529	-168.288373	-168.285484	-168.300328
NH ₃	-56.415524	-56.422829	-56.399747	-56.407053
cyanic acid + NH ₃	-224.689073	-224.711202	-224.685231	-224.7073560
cyanate	-167.757603	-167.860627	-167.779818	-167.882842
NH ₄ ⁺	-56.755685	-56.889853	-56.725201	-56.859367
cyanate + NH ₄ ⁺	-224.513288	-224.750478	-224.505019	-224.742209

^a (MP2/6-311++G** level of theory) for the species involved in the different steps of the reaction shown in Figure 2.

Table 4. Relevant Structural Parameters (Interatomic Distances in Å, Angles in Degrees)^a

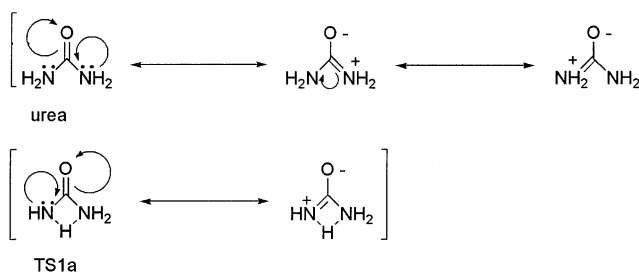
	r _{CO}	r _{CN1}	r _{CN2}	r _{N1H1}	r _{OH1}	r _{N1H2}	r _{N2H2}	<N ₁ HN ₂
urea	1.218	1.391	1.391	1.010	2.462	2.487	1.010	68.8
TS2a	1.293	1.323	1.361	1.571	1.015	1.013	2.770	59.9
I2a	1.357	1.279	1.376	2.250	0.966	1.018	2.553	69.9
TS2b	1.367	1.241	1.537	2.553	0.966	1.543	1.208	111.1
cyanic acid	1.304	1.176			0.965			

^a For the elimination reaction pathway shown in Figure 2.

by the second transition state found along the reaction path (TS_{2b}). This elimination mechanism leads to cyanic acid (and ammonia), instead of the isocyanic acid isomer experimentally found. The conversion of cyanic to isocyanic acid cannot proceed by means of intramolecular H-transfer because the barrier height is extremely high and the reaction is formally disallowed by the Woodward–Hoffmann rules. In agreement with previous data,^{17,18} we found that the isomerization can readily proceed in aqueous media through hydrated intermediates. Nonetheless, this reaction is not necessary in this case, because the proton can be transferred to ammonia to give the same products as shown in Figure 1, in a process that is favored when solvation is included.

This elimination mechanism, in the reverse direction, was analyzed as a possible step in the mechanism of the Wohler synthesis.¹⁷ As in the previous case, similar TS structures were found, but higher energy requirements were calculated. The reaction was also predicted to be exothermic, while we found that this is true only when solvent is ignored. The structural characteristics of stable intermediates and transition states are summarized in Table 4.

The electronic structures of urea and its derivatives have been studied extensively with regard to the factors that influence its resonance stabilization.²⁸ In the elimination reaction pathway, the resonance of urea is clearly disrupted. The hybridization of the amide N atoms changes from a mixed sp²–sp³ electronic configurations to sp² hybridization on the H-donor atom and sp³ on the H-acceptor atom. The change is reflected in the decrease and elongation of the associated C–N bonds (Table 1). In TS_{1a}, the migrating proton is at the midway point between the two amide nitrogen atoms. To attain this coordination, the NCN angle decreases from 113° to 94°, at the expense of an increase of the OCN₁ angle to 140°. The structure can be described as a distorted isocyanic acid, where an ammonia molecule is coordinated to the C atom. In this way, the electron delocalization, which in the urea molecule extends over four

Scheme 1

atomic centers, is restricted to three atoms in TS_{1a} (Scheme 1). A similar effect is responsible for the increase in the energy when going from I_{2a} to TS_{2b}.

3.2. One-Water-Assisted Decomposition of Urea. Solvent participation in the decomposition of urea has been considered a strong possibility since the initial kinetic studies of urea in aqueous media.^{8,9,29} Among the different water–urea coordination geometries that can be proposed, we have chosen to analyze the most stable ones in detail, which involve H-bonding of water either to the carbonyl oxygen and one nitrogen atom or to both nitrogen atoms of the urea molecule (Figures 3 and 4). These two coordination modes were computed to be nearly isoenergetic. Inclusion of solvent is relevant in these cases, because not unexpectedly, the urea–water complexes were calculated to be more stable than the separated species in vacuo, while the formation of the complexes was endothermic when solvation was included (Tables 5 and 6).

The coordination mode of water that involves forming hydrogen bonds with the carbonyl and a nitrogen atom (ureaw3 in Figure 3) has a free energy of formation that is uphill by 8 kcal/mol (Table 5). The increase in the free energy originates from an entropic effect: from the energy differences, an exothermic reaction would be predicted. The resulting complex facilitates the nucleophilic attack of the oxygen–water (OW) on the carbonyl carbon atom, giving a transition state (TS_{3a}) in which the oxygen is 2.0 Å away from the carbon, and the urea molecule is slightly distorted from planarity (the sum of the X–C–Y angles around the C atom is 353°). In TS_{3a} one of the hydrogen atoms of water (HW) has been transferred to the carbonyl oxygen. From this structure, the tetrahedral intermediate I_{3a} is easily generated via bond formation between the carbonyl carbon and the water oxygen. The free energy of activation for this reaction is close to 55 kcal/mol. I_{3a} can then undergo two possible reactions. Via a proton transfer, from the OH group to one of the NH₂ groups (via TS_{3b}), carbamic acid

(27) Lynch, B. J.; Truhlar, D. G. *J. Phys. Chem. A* **2001**, *105*, 2936.

(28) Bharatam, P. V.; Moudgil, R.; Kaur, D. *J. Phys. Chem. A* **2003**, *107*, 1627.

(29) Yankwich, P. E.; Veazie, A. E. *J. Am. Chem. Soc.* **1958**, *80*, 1835.

Table 5. Electronic (E, au) and Free Energies (G, au, 298 K, 1 bar) Derived from Gas Phase and ICPM (Solvent = Water) Calculations^a

	E gas phase (au)	E solvent	G gas phase (au)	G solvent
urea	-224.756496	-224.772684	-224.718067	-224.734255
water	-76.233376	-76.285889	-76.229393	-76.281906
urea + water	-300.989872	-301.058579	-300.947460	-301.016160
ureaw3	-301.046985	-301.064666	-300.985252	-301.002670
TS3a	-300.961635	-300.986076	-300.903638	-300.928079
I3a	-301.015034	-301.032016	-300.950528	-300.967510
TS3b	-301.010700	-301.029500	-300.946779	-300.965579
carbamic acid	-244.603798	-244.623035	-244.588224	-244.607461
carbamic + NH ₃	-301.019322	-301.045863	-301.008395	-301.014513
carbamate	-244.051454	-244.159882	-244.048510	-244.156939
carbamate + NH ₄ ⁺	-300.807139	-301.049732	-300.773711	-301.016304
TS3c	-301.011732	-301.029220	-300.948083	-300.965571
NH ₃	-56.415524	-56.422829	-56.399747	-56.407053
I3b	-244.584224	-244.596272	-244.559074	-244.571122
I3b + NH ₃	-300.999748	-301.019100	-300.958821	-300.978173
TS3d	-244.545545	-244.558126	-244.541836	-244.553884
TS3d + NH ₃	-300.961069	-300.980956	-300.941583	-300.961469
I3c	-244.590934	-244.604031	-244.588723	-244.601820
I3c + NH ₃	-301.006458	-301.026860	-300.988470	-301.008873
NH ₄ ⁺	-56.755685	-56.889853	-56.7252001	-56.859367
I3d	-244.061845	-244.156931	-244.164903	-244.164903
I3d + NH ₄ ⁺	-300.817531	-301.046781	-300.795018	-301.024261

^a (MP2/6-311++G** level of theory) for the species involved in the different steps of the reaction shown in Figure 3.

Table 6. Electronic (E, au) and Free Energies (G, au, 298 K, 1 bar) Derived from Gas Phase and ICPM (Solvent = Water) Calculations^a

	E gas phase	E solvent	G gas phase (au)	G solvent
urea	-224.756496	-224.772684	-224.718067	-224.734255
water	-76.233376	-76.285889	-76.229393	-76.281906
urea + water	-300.989872	-301.058579	-300.947460	-301.016160
ureaw4	-301.042662	-301.065921	-300.986389	-301.009648
TS4a	-301.003419	-301.029485	-300.946718	-300.972783
NH ₃	-56.415524	-56.422829	-56.399747	-56.407053
isocyanic acid	-168.311859	-168.318144	-168.323607	-168.329892
isocyanic acid + H ₂ O	-244.590934	-244.604031	-244.588723	-244.601820
isocyanic + NH ₃ + H ₂ O	-301.006458	-301.026860	-300.988470	-301.008873
NH ₄ ⁺	-56.755685	-56.889853	-56.7252001	-56.859367
isocyanate	-167.757603	-167.860627	-167.779818	-167.882842
cyanate + H ₂ O	-244.061845	-244.156931	-244.164903	-244.164903
cyanate + NH ₄ ⁺ + H ₂ O	-300.817531	-301.046781	-300.795018	-301.024261

^a (MP2/6-311++G** level of theory) for the species involved in the different steps of the reaction shown in Figure 4.

Table 7. Relevant Structural Parameters (Interatomic Distances, Å)^a

	r _{CO}	r _{CN1}	r _{CN2}	r _{OHW}	r _{OHW2}	r _{OWC}	r _{OWHW}	r _{HWN1}	r _{HIN1}
ureaw3	1.229	1.386	1.377	1.907	2.068	3.218	0.972	3.521	3.196
TS3a	1.326	1.364	1.360	1.064	2.643	2.006	1.401	2.688	3.208
I3a	1.404	1.440	1.440	0.964	2.625	1.415	2.130	2.739	3.200
TS3b	1.420	1.442	1.430	0.963	2.505	1.404	2.681	2.300	2.460
TS3c	1.401	1.449	1.439	0.963	2.393	1.406	2.279		
I3b	1.356	1.229		0.963		1.382	2.107		
TS3d	1.356	1.230		0.965		1.381	1.778		
I3c	1.176	1.220		2.151		4.096	0.962		
I3d	1.240	1.200		1.779		3.769	0.980		
carbamic acid	1.203		1.391		0.962	1.363			
carbamate	1.255		1.468			1.255			

^a Calculated at the MP2/6-311++G** level for the different steps of the elimination reaction pathway shown in Figure 3a,b.

and ammonia can be readily generated (Figure 3a). The conversion of I_{3a} into isocyanic acid (Figure 3b) has a larger ΔG_{act} associated with it. It follows a mechanism that involves proton transfer between both NH₂ groups and proceeds through a gem-diol-like transition state (TS_{3c}). Thus, this solvent binding mode favors the formation of carbamic over isocyanic acid as the main reaction product, closely resembling the urease-catalyzed process. Relevant structural details for the different steps of the reaction are reported in Table 7.

The second hydrogen bonding mode (ureaw4; Figure 4), which is uphill in free energy by 4 kcal/mol, facilitates

intermolecular proton transfer, lowering the ΔG_{act} to 27 kcal/mol, while directly forming the experimentally observed products. The transition state (TS_{4a}) is a six-membered ring formed of N–H and O–H hydrogen bonds, where one HW has been transferred to the amide nitrogen which elongates the C–N distance to 1.55 Å (Table 8). This amide nitrogen is then subsequently released as NH₃.

In the Wohler synthesis a similar TS was found,¹⁷ which is a preliminary step in the addition of NH₃ to the C=N bond of isocyanic acid, assisted by a water molecule hydrogen-bonded to NH₃. Although a similar six-member TS was reported, the

Table 8. Relevant Structural Parameters (Interatomic Distances Å)^a

	r_{CO}	r_{CN1}	r_{CN2}	r_{OWH1}	r_{OWH2}	r_{N2HW}	r_{N1H1}	r_{N2H2}
ureaw4	1.222	1.386	1.386	2.225	2.225	3.626	1.011	1.011
TS4a	1.272	1.603	1.603	3.462	0.956	2.423	1.004	2.001

^a Calculated at the MP2/6-311++G** level for the different steps of the elimination reaction pathway shown in Figure 4.

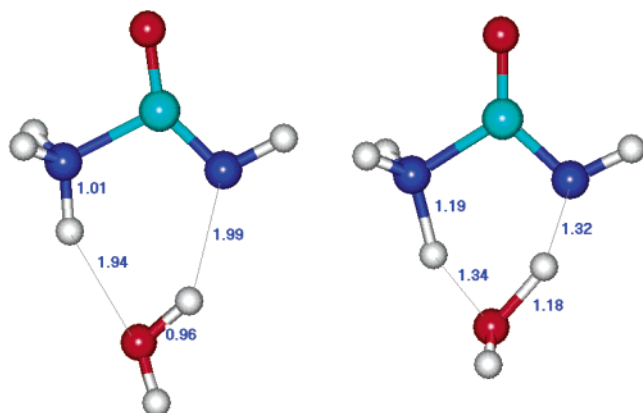


Figure 5. Structural characteristics of the TS in the elimination reaction assisted by one water molecule, calculated at the MP2/6-311++G** level (left) and B3LYP/6-31G** level.

reported N–H–O hydrogen bonds distances are significantly different than observed herein. For example, the X–H–Y distances, which are close to 1.35 Å at the B3LYP/6-31G** level, elongate to 1.9 Å at the MP2/6-311++G** level of theory (Figure 5). Moreover, the energies calculated for consecutive steps of the urea synthesis were not solvent-corrected and lead to the prediction of an exothermic reaction, while we predict that the energy decreases in the reverse direction.

Despite the participation of a water molecule, the bond lengths are similar in TS_{1a} and TS_{4a} (Tables 1 and 8). Nevertheless, TS_{4a} is closer to products than TS_{1a}, with a CN bond distance 2% longer in the former. TS_{4a} can be also described as a distorted isocyanic acid, where the NH₃ molecule, coordinated

to the C atom, is H-bonded to a water molecule. The water molecule helps to lower the energy of TS_{4a}, relative to TS_{1a}, as it allows hydrogen transfer to proceed with a smaller NCN angular distortion. This angle retains a value of 109°, close to the one found in urea. The increase of the OCN₁ angle to 142° occurs at the expense of the OCN₂ one, which decreases to 110°. As was previously discussed for TS_{1a}, electron delocalization, which in the urea molecule extends over four atomic centers, is restricted in TS_{4a}, to the three atoms of the isocyanic acid moiety. In TS_{3a}, on the other hand, the resonance stabilization is disrupted, as the central C atom is at the van der Waals distance of OW, stabilizing a quasi-tetrahedral geometry, with large sp³ contribution to the C atom hybridization.

3.3. Two-Water-Assisted Decomposition of Urea. Water assistance could involve the coordination of several water molecules to a single urea molecule, in a manner and number not easily predictable. To assess how extra water molecules might affect the reaction pathway, we have extended our analysis to the case in which two water molecules simultaneously assist the reaction. Two favorable water coordination modes are shown in Figures 6 (ureaw5) and in 7 (ureaw6), which are calculated to be isoenergetic at the MP2/6-311++G** level. The two coordination modes differ with respect to the hydrogen bonds they form with urea. The structure of Figure 7 hydrogen bonds with only the amide groups, while the structure of Figure 6 hydrogen bonds with both the amide and carbonyl groups of the urea molecule. Solvent corrections favor the structure of Figure 7 by 3.7 kcal/mol over the structure shown in Figure 6.

The hydrogen-bonding pattern shown in Figure 6 (ureaw5) is 17 kcal/mol uphill in free energy (Table 9) and leads to the products of the catalyzed hydrolysis (cyanic acid and ammonium). The reaction mechanism involves two transition-state structures. The first one (TS_{5a}) is associated with a change in the coordination mode of one of the water molecules. TS_{5b} generates a hydroxide ion via a series of proton transfers, which then attacks the carbonyl carbon of urea generating a gem-diol intermediate. The generation of a hydroxide ion around urea and its subsequent attack at the carbonyl carbon defines the rate-

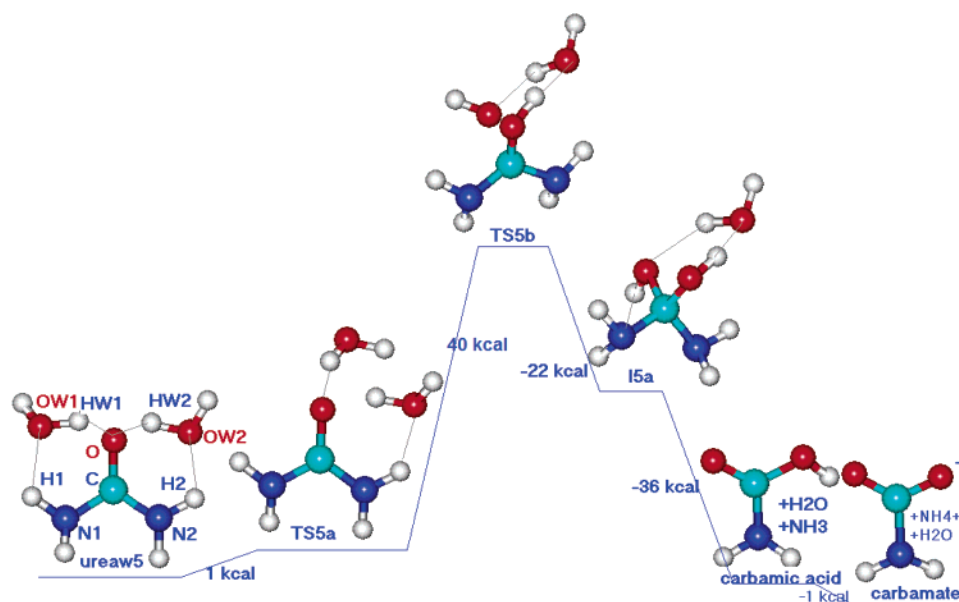


Figure 6. Reaction profile for the urea hydrolytic decomposition pathway assisted by two water molecules, leading to carbamic acid. ΔG_{act} values, calculated at the MP2/6-311++G** level, are solvent-corrected. Relative energies are not drawn to scale.

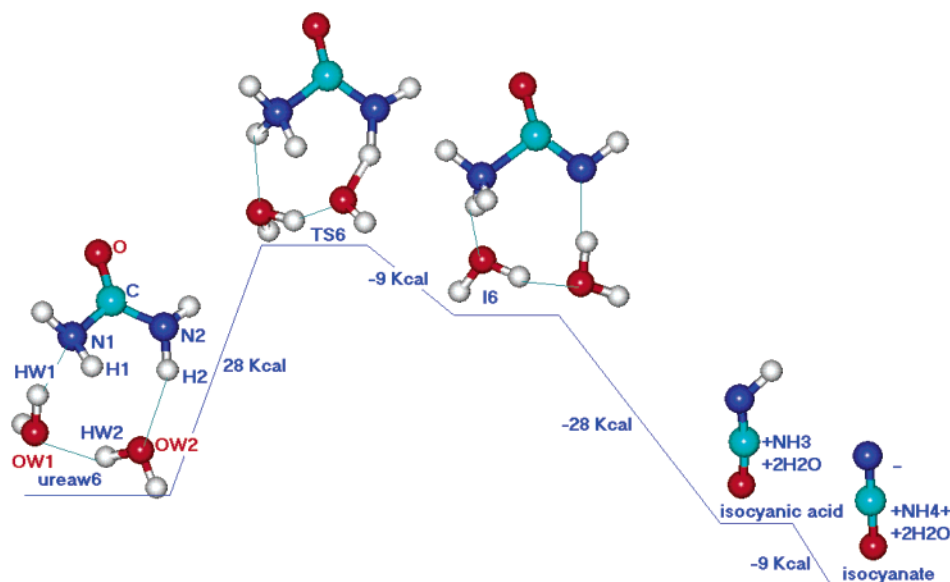


Figure 7. Reaction profile for the urea elimination decomposition pathway assisted by two water molecules, leading to isocyanic acid. ΔG_{act} values, calculated at the MP2/6-311++G** level, are solvent-corrected. Relative energies are not drawn to scale.

Table 9. Electronic (E, au) and Free Energies (G, au, 298 K, 1 bar) Derived from Gas Phase and ICPM (Solvent = Water) Calculations^a

	E gas phase (au)	E solvent (au)	G gas phase (au)	G solvent
urea	-224.756496	-224.772684	-224.718067	-224.734255
water	-76.233376	-76.285889	-76.229393	-76.281906
urea + 2 water	-377.223246	-377.351413	-377.176850	-377.298064
ureaw5	-377.331182	-377.351413	-377.257413	-377.271441
TS5a	-377.331182	-377.349005	-377.252300	-377.270123
TS5b	-377.269331	-377.289392	-377.186736	-377.206797
I5b	-377.305033	-377.327164	-377.218719	-377.240851
NH ₃	-56.415524	-56.422829	-56.399747	-56.407053
carbamic acid	-244.603798	-244.623035	-244.588224	-244.607461
carb + NH ₃ + water	-377.250566	-377.331753	-377.217783	-377.298923
NH ₄ ⁺	-56.755685	-56.889853	-56.7252001	-56.859367
carbamate	-244.051454	-244.159882	-244.048510	-244.156939
Carbm + NH ₄ ⁺ + water	-377.040515	-377.335621	-377.003104	-377.298200

^a (MP2/6-311++G** level of theory) for the species involved in the different steps of the reaction shown in Figure 6.

Table 10. Relevant Structural Parameters (Interatomic Distances, Å)^a

	r_{CO}	r_{CN1}	r_{CN2}	r_{H1OW1}	r_{H1O}	r_{OW1O}	r_{OW2HW1}	r_{OW1HW2}	r_{OW1C}
ureaw5	1.240	1.372	1.372	2.060	1.908	2.790	4.551	4.551	3.236
TS5a	1.209	1.362	1.353	4.709	2.133	3.035	3.243	3.087	3.887
I5a	1.292	1.338	1.344	2.974	0.962	2.658	1.804	1.600	2.146
TS5b	1.447	1.427	1.443	2.652	0.970	2.262	1.944	1.974	1.447

^a Calculated at the MP2/6-311++G** level for the different steps of the elimination reaction pathway shown in Figure 6.

determining step (ΔG_{act} of 56 kcal/mol including 17 kcal/mol for the free energy of association), which has similar ΔG_{act} to that calculated for the related reaction shown in Figure 3. From TS_{5b}, the stable intermediate I_{5a} is formed, which can then readily collapse to form ammonia and carbamic acid. The main structural characteristics of the intermediates that develop in the different stages of the reaction are given in Table 10. The structure of TS_{5b} is very close to that of TS_{3a}, showing the same distorted geometry of the urea molecule, triggered by the coordination of the OH to the C atom. According to the respective activation energies, the second water molecule does not seem to be relevant for the progress of the reaction. The structural similarity extends to the gem-diol intermediate (I_{5a}), which can be superimposed with I₃ (Figure 3), when the additional water molecule H-bonded to the hydroxyl groups is disregarded.

Ureaw6 proceeds through TS₆ (Figure 7), which precedes the elimination reaction. The elimination mechanism that occurs from this coordination mode has a free-energy barrier of 41 kcal/mol (including the association free energy; Table 11). TS₆ is the rate-determining step that has a N–C interatomic distance of 1.54 Å, characteristic of a single bond, that further elongates to 1.64 Å to yield an intermediate (I₆), where the NH₃ molecule has nearly dissociated from urea, leaving the OCNH moiety that ultimately rearranges to isocyanic acid (Table 12). The geometry of the urea moiety in TS₆ is similar to that of TS₄ (they can also be superimposed if the second water molecule is disregarded). The presence of the second water molecule does not help in lowering the free energy of activation, relative to the participation of a single water molecule in the reaction.

A similar coordination mode and associated TS structures have been previously considered in the theoretical study of the

Table 11. Electronic (E, au) and Free Energies (G, au, 298 K, 1 bar) Derived from Gas Phase and ICPM (Solvent = Water) Calculations^a

	E gas phase (au)	E solvent (au)	G gas phase (au)	G solvent
urea	-224.756496	-224.772684	-224.718067	-224.734255
water	-76.233376	-76.285889	-76.229393	-76.281906
urea +2 water	-377.223246	-377.351413	-377.176850	-377.298064
ureaw6	-377.338002	-377.358756	-377.256781	-377.277538
TS6	-377.290981	-377.312616	-377.211819	-377.233455
I6	-377.299117	-377.327370	-377.219259	-377.247461
NH3	-56.415524	-56.422829	-56.399747	-56.407053
isocyanic acid	-168.311859	-168.318144	-168.323607	-168.329892
isocyanic acid + 2H ₂ O	-320.824310	-320.889920	-320.818116	-320.883726
isocyanic acid + NH ₃ + 2H ₂ O	-377.239834	-377.312749	-377.217863	-377.290779
NH ₄ ⁺	-56.755685	-56.889853	-56.7252001	-56.859367
isocyanate	-167.757603	-167.860627	-167.779818	-167.882842
cyanate + 2H ₂ O	-320.295221	-320.442820	-320.394296	-320.446809
cyanate + NH ₄ ⁺ + 2H ₂ O	-377.050907	-377.332670	-377.024474	-377.306167

^a (MP2/6-311++G** level of theory) for the species involved in the different steps of the reaction shown in Figure 7.

Table 12. Relevant Structural Parameters (Interatomic Distances, Å)^a

	r _{CO}	r _{CN1}	r _{CN2}	r _{HN1N1}	r _{H2OW2}	r _{HW2OW1}	r _{N2H2}	r _{HW1OW1}	r _{HW2OW2}
ureaw6	1.221	1.413	1.371	1.994	2.006	1.864	1.014	0.974	0.973
TS6	1.215	1.541	1.322	1.033	1.301	0.986	1.193	1.918	1.739
I6	1.219	1.614	1.305	1.041	0.995	0.981	1.750	1.753	1.745

^a Calculated at the MP2/6-311++G** level for the different steps of the elimination reaction pathway shown in Figure 7.

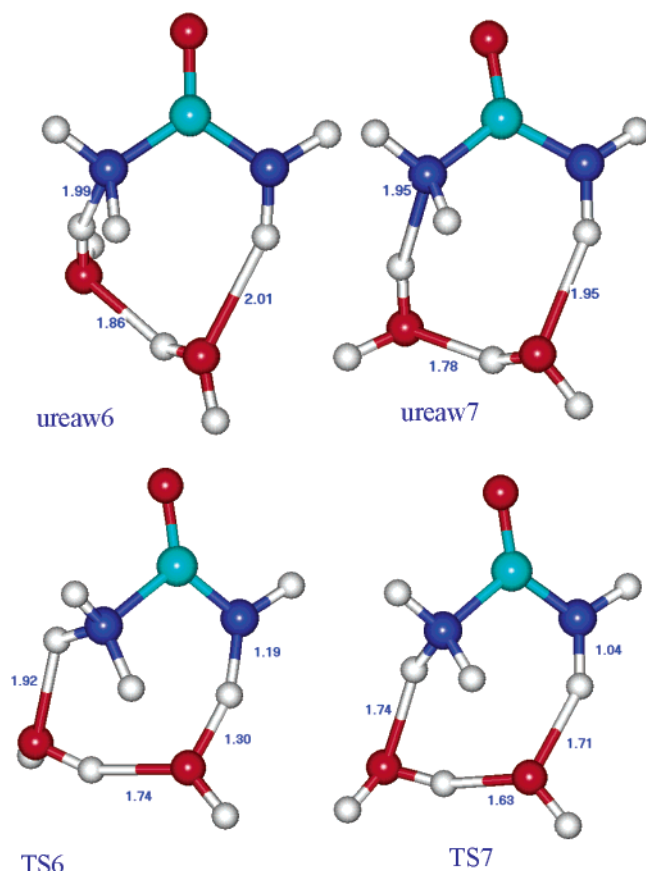


Figure 8. Structural characteristics of the stable adducts and TS for the two-water-assisted reaction, calculated at the MP2/6-311++G** level (ureaw6, TS6) and B3LYP/6-31+G* level (ureaw7, TS7).

Wohler reaction. In this case, however, the reaction was for a water dimer-assisted addition of NH₃ to the C=N double bond of HNCO. The reported structure (ureaw7; Figure 8) differs from ours in the relative orientation of the non-bonded H atom of one of the water molecules. To further understand the potential energy surface of this reaction, we have optimized ureaw6 at

the B3LYP/6-31+G* level and ureaw7 at the MP2/6-311++G** level of theory. We found that the B3LYP/6-31+G* calculations identified two different nearly isoenergetic minima, but both structures converged to ureaw6 at higher levels of theory (MP2/6-311++G**). The details for the stable species and TS structures that we found at each computational level are compared in Figure 8.

3.4. Kinetic Analysis of the Elimination Reaction. In this section, we present a detailed analysis of the kinetics of the elimination reaction, for which experimental data are available^{8–10,29} According to our calculations, the one-water-assisted mechanism (Figure 4) is favored for the uncatalyzed elimination reaction in aqueous solution. To obtain calculated kinetic parameters useful to validate the proposed mechanism against available experimental data, we have used our calculated thermodynamic functions (G, S, H) in conjunction with standard activated complex theory.

The elimination reaction is first-order in urea, with rate constants of $4.15 \times 10^{-5} \text{ s}^{-1}$ at 373.15 K and $2.09 \times 10^{-7} \text{ s}^{-1}$ at 333.15 K, measured in 0.05 M H₂SO₄. The reaction rate constant in water is of the same order of magnitude as that in acid.³⁰ Nevertheless, a tendency has been reported for the rate constant in acid to be higher, and it has been associated with the occurrence of reverse reactions in water, which cause a deviation from linearity in the plots of reaction rate vs concentration.³⁰ We will discuss this observation in the following paragraphs, on the basis of our calculated data.

We first focus on deriving kinetic data for the reaction mechanism shown in Figure 4. We compute rate constants k of $1.5 \times 10^{-5} \text{ s}^{-1}$ at 373.15 K ($\Delta G_{\text{act}} = 29.9 \text{ kcal/mol}$), and $4.9 \times 10^{-7} \text{ s}^{-1}$ at 333.15 K ($\Delta G_{\text{act}} = 28.8 \text{ kcal/mol}$), in excellent agreement with the experimental data. Calculated and experimental rate constants are compared in Table 13. From these data, the activation energy can be easily evaluated from the slope of an Eyring plot ($\ln k$ vs $1/T$). Despite the good agreement between the rate constants, the activation energy is underesti-

(30) Shaw, W. H.; Bordeaux, J. J. *J. Am. Chem. Soc.* **1955**, *27*, 4729.

Table 13. Experimental (k_{exp} , ref 30) and Calculated (k_{calcd}) First-Order Rate Constants for the Decomposition of Urea^a

T [K]	$k_{\text{exp}} \times 10^{-5} \text{ s}^{-1}$	$k_{\text{calcd}} \times 10^{-5} \text{ s}^{-1}$	$k_{\text{Hcalcd}} \times 10^{-5} \text{ s}^{-1}$
333.15	0.0207	0.045	0.079
343.15	0.083	0.150	0.240
353.15	0.385	0.282	0.724
363.15	1.20	0.525	2.089
373.25	4.15	1.59	6.30

^a k_{Hcalcd} refers to the data calculated in acid media, according to the reaction pathway shown in Figure 9.

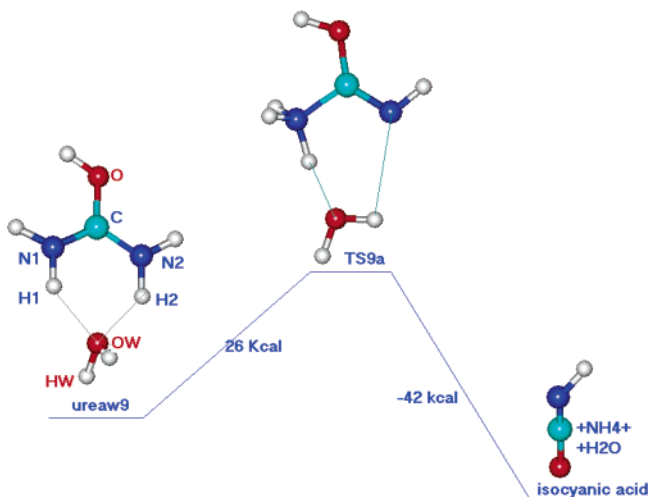


Figure 9. Reaction profile for urea elimination pathway in acid media, assisted by one water molecule, leading to isocyanic acid. ΔG_{act} values, calculated at the MP2/6-311++G** level, are solvent-corrected. Relative energies are not drawn to scale.

mated. We calculate a value of 19 kcal/mol, compared to an experimental value of 32.7 kcal/mol. The latter has been derived from the plot of the experimental rate constants, obtained for temperatures ranging from 333.15 to 373.15 K.³⁰

According to the available experimental data, the reaction rate can be represented by the equation¹³

$$v = k_1'[\text{urea}] = k_1[\text{urea}][\text{H}_3\text{O}^+]$$

where k_1' is the pseudo-first-order constant and k_1 is a second-order constant. On the other hand, it is well-known that the hydrolysis of amide functional groups at low pH involves water attack to the O-protonated amide.^{31,32} Hence, to properly model the influence of the acid media, we have performed similar calculations for the reaction shown in Figure 9, where the carbonyl oxygen of the urea molecule is protonated. The associated reaction rate is calculated from the equation

$$v = k_2[\text{urea}^+][\text{H}_2\text{O}] = k_2'[\text{urea}^+]$$

The calculated ΔG_{act} for the reaction (Figure 9) is not strongly affected by protonation (Tables 6 and 14). Nevertheless, the electronic characteristics of the intermediates are certainly different. Protonation of the carbonyl prevents the electron delocalization from extending to this group. Delocalization is only associated with the lone pairs on the amide nitrogen atoms (and CN bonds), resulting in planar structures (sp^2) around these

centers. This description agrees with a large relative weight for the charged structures in the resonance picture of the urea molecule.²⁸ The larger sp^2 contribution is reflected in shortened C–N bonds (0.5%) and a higher energy required for proton transfer (Table 15). From the Eyring plot of the reaction rate constants derived for this reaction an activation energy of 31.6 kcal/mol is calculated, in excellent agreement with the experiment (Table 13). This agreement increases our confidence in our calculated data for other reaction pathways, discussed below, for which experimental data are not available.

The lack of occurrence of reverse reactions in acid media has been explained on the basis of an ionic mechanism for urea decomposition, which also helps to explain the increase of the reaction rate due to the higher ionic strength of the acid solution.³⁰ Our calculations show a significant weight of ionic contributions to the resonance structure of the protonated urea molecule that properly model the elimination kinetics, providing further support to this extensively discussed possible mechanism.³⁰

3.5. Mechanism of the Catalyzed Hydrolysis. The Proficiency of Urease. The mechanisms described above provide valuable insights that allow us to better understand the probable reaction paths that occur in solution or in the active site of urease. As discussed in the previous section, the mechanism shown in Figure 4 is the most favored in solution and leads to the experimentally found elimination products. In the enzyme active site, however, urea coordination involves hydrogen bonding with key residues of the protein, located in a mobile flap,¹ precluding the coordination of a water molecule as it occurs in ureaw4. Preliminary results of molecular dynamics (MD) simulations³³ point to Cys319, His320, and Ala167 as relevant for catalysis (Figure 10). Hydrogen bond coordination to these residues can be attained for the closed conformation of the mobile flap. In addition, the MD simulations show that the urea oxygen atom is hydrogen-bonded to the hydroxide ion that is bridging the dinickel cluster in the active site of urease, while the hydroxyl oxygen hydrogen bonds to a hydrogen atom from one of the amide groups of urea. This coordination motif closely resembles that of ureaw3, since the two urea structures can be superimposed (Figure 11). A similar coordination mode has been found in recent ab initio calculations of the interaction of urea with cluster models of the urease active site.³⁴ This optimized structure, shown in Figure 12, also overlaps with the ureaw3 structure.

The preliminary results of the MD simulations are also in agreement with the coordination involved in the first stage of the reaction mechanism suggested by Karplus¹ (Figure 13) for the urease-catalyzed hydrolysis. In this mechanism, the major kinetic barrier was assigned to a step in which the hydroxide bound to the dinickel active site center attacks the carbonyl carbon of urea to form a tetrahedral hydrated urea TS,¹ which further generates an intermediate similar to I3. This coordination mode impedes the uncatalyzed mechanism that we have calculated with the lowest ΔG_{act} , which, indeed, is an elimination reaction (Figure 4). The elimination reaction has not been thought to occur in the enzyme active site. Similarly, the two-water-assisted reaction of Figure 6 would not be favored since

(31) Zahn, D. *J. Phys. Chem. B* **2003**, *10*, 12303.

(32) Brown, R. S.; Bennet, A. J.; Slebocka-Tilk, H. *Acc. Chem. Res.* **1992**, *25*, 481.

(33) Estiu, G. L.; Merz, K. M. Manuscript in preparation.

(34) Suarez, D.; Diaz, N.; Merz, K. M. *J. Am. Chem. Soc.* **2003**, *125*, 15324.

Table 14. Electronic (E, au) and Free Energies (G, au, 298 K, 1 bar) Derived from Gas Phase and ICPM (Solvent = Water) Calculations^a

	E gas phase	E solvent	G gas phase (au)	G solvent
ureap	-225.095142	-225.208865	-225.045450	-225.159173
water	-76.233376	-76.285889	-76.229393	-76.281906
ureap + water	-301.328518	-301.494754	-301.274852	-301.441088
ureaw9	-301.402175	-301.502489	-301.331495	-301.431809
TS9	-301.350474	-301.468681	-301.280868	-301.399074
NH ₄ ⁺	-56.755685	-56.889853	-56.7252001	-56.859367
isocyanic acid	-168.311859	-168.318144	-168.323607	-168.329892
isocyanic acid + H ₂ O	-244.590934	-244.604031	-244.588723	-244.601820
isocyanic + NH ₄ ⁺ + H ₂ O	-301.346619	-301.493884	-301.312923	-301.461187

^a (MP2/6-311++G** level of theory) for the species involved in the different steps of the reaction shown in Figure 9.

Table 15. Relevant Structural Parameters (Interatomic Distances, Å)^a

	r _{CO}	r _{CN1}	r _{CN2}	r _{OWH1}	r _{OWH2}	r _{N1HW}	r _{N1H1}	r _{N2H2}
ureaw9	1.315	1.326	1.318	1.990	2.036	3.279	1.019	1.016
TS9a	1.333	1.489	1.257	3.090	0.968	1.078	1.021	2.678

^a Calculated at the MP2/6-311++G** level for the different steps of the elimination reaction pathway shown in Figure 9.

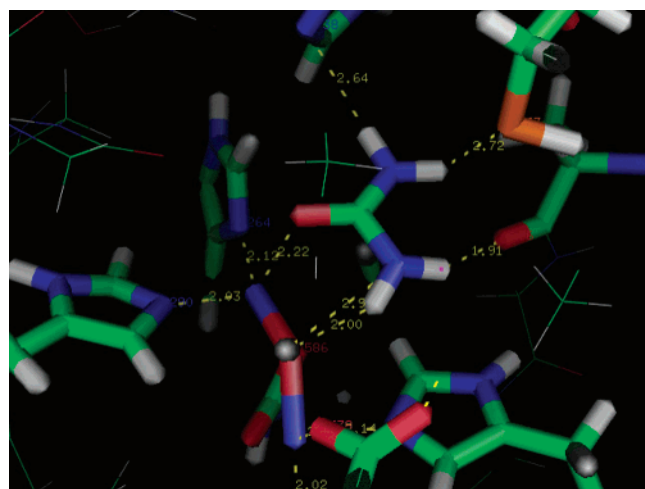


Figure 10. Coordination of urea to the active site of urease, after a 1 ns MD simulation. The initial model has been built by docking urea into the active site of 3UBP.^{35,36,43} H-bond coordination to key residues of the mobile flap are shown, as well as the interactions with the dinickel bridging OH.

two of the four urea protons would need to be complexed by water molecules.

The process shown in Figure 3, describing nucleophilic attack on the carbonyl carbon atom by a water molecule, appears to be the pathway that is most consistent with what might occur within the active site of urease. The similarity of the mechanism proposed in Figure 3 and the one proposed for urease hydrolysis (Figure 13) is remarkable. Our calculations predict a large ΔG_{act} (55 kcal/mol) for this mechanism. Nevertheless, coordination of urea to the active site would certainly lower its resonance stabilization and, hence, the associated ΔG_{act} .

The kinetic parameters for the uncatalyzed hydrolysis reaction have never been determined, since, as noted, this reaction proceeds via elimination in the absence of urease. From our computations, we are now capable of obtaining the value of the rate constant for the hydrolytic reaction described in Figure 3, on the basis of our calculated thermodynamic data. The value, $2.5 \times 10^{-27} \text{ s}^{-1}$ at 310.15 K, characterizes extremely slow reaction kinetics. In the urease active site, the hydrolysis occurs 10^{14} times faster than the noncatalyzed elimination reaction, according to available experimental data.¹ The rate constant for the enzymatic hydrolysis of urea at 310.15 K is $3.5 \times 10^3 \text{ s}^{-1}$

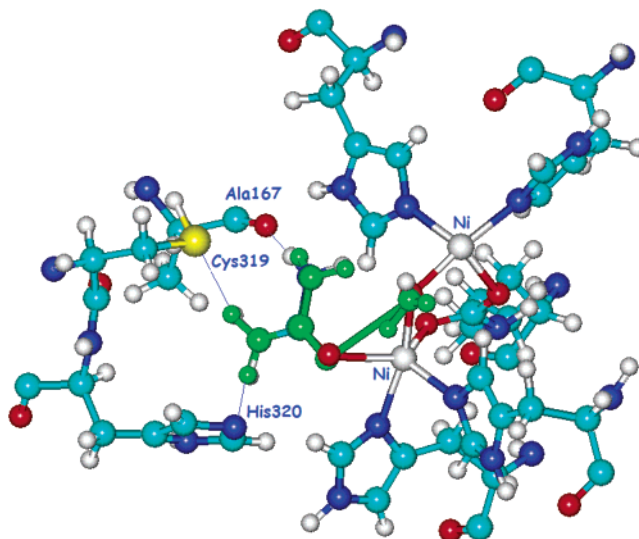


Figure 11. Superposition of ureaw3 (in green) with the urea moiety bound to the active site of the protein structure shown in Figure 10. Only the residues coordinated to the Ni atoms and those H-bond-coordinated to urea have been kept for clarity.

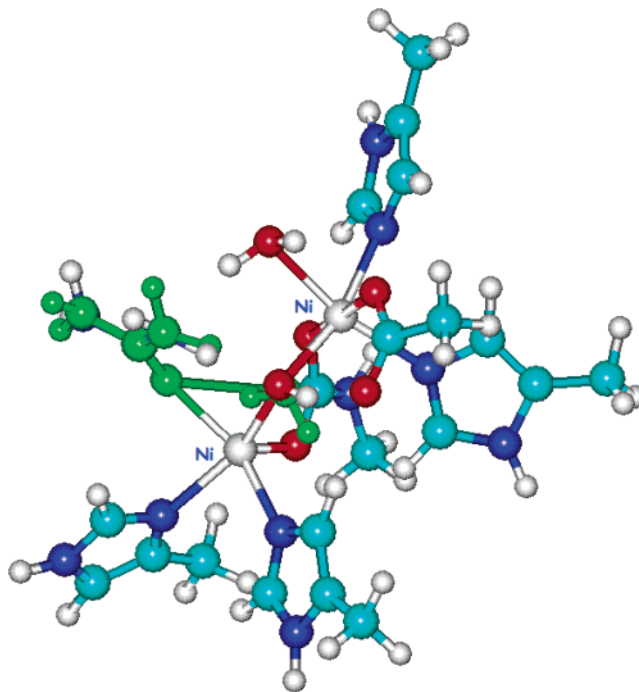


Figure 12. Superposition of ureaw3 (in green) with the urea moiety of the structure that results from ab initio calculations of cluster models of the active site (from ref 34).

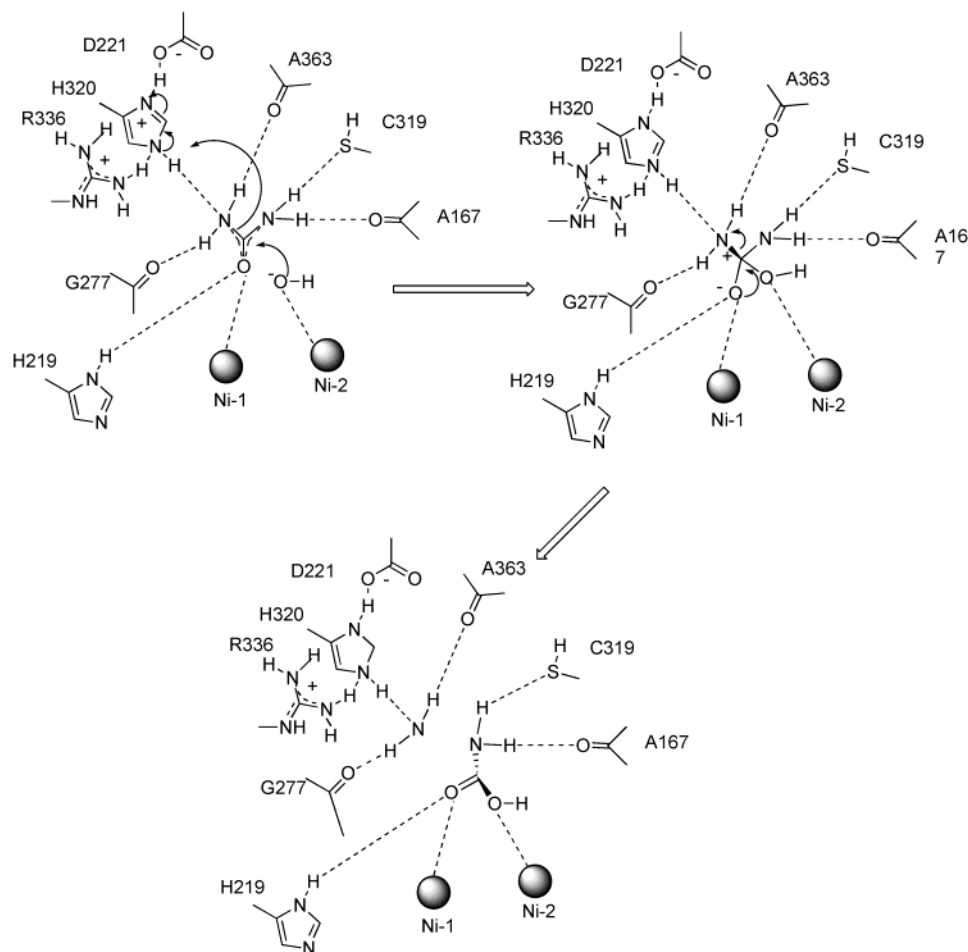


Figure 13. Structurally detailed mechanism for urease catalysis proposed in ref 15. The elimination reaction proceeds through a tetrahedral intermediate that closely resembles I3a (Figure 3a).

in *Klebsiella aerogenes* urease, which has a K_m for urea of 2.5×10^{-3} M.⁵ Comparing our computed rate for the uncatalyzed hydrolysis reaction indicates that the enzyme actually attains a 10^{30} fold increase in the reaction rate for the hydrolytic decomposition.

An enzyme's proficiency as a catalyst can be evaluated by dividing k_{cat}/K_m by the rate constant for the same reaction, measured in neutral aqueous solution, in the absence of the enzyme (k_{non}).¹⁴ Catalytic proficiency, defined in this way, measures an enzyme's ability to lower the activation barrier for the reaction of a substrate in solution. Urease proficiency has never been evaluated before, because the catalyzed and uncatalyzed reactions follow different reaction mechanisms. Thus, theoretical tools can be used to better align what is thought to be occurring in the enzyme (hydrolysis) with the disfavored or unobserved reaction in solution (elimination versus hydrolysis). The resulting calculated k_{non} value allows us to evaluate, for the first time, the proficiency of urease in a manner consistent with other enzyme systems.^{13,14}

The theoretical calculations are not only helpful to evaluate the catalytic proficiency, but also to understand the most significant features that help to reduce the activation energy in the enzyme active site. According to our model, polarization of the carbonyl group appears to be the key issue (Figure 3). This is achieved (Figure 10) through coordination of the urea protons to electron-withdrawing groups, which activate the carbon atom toward nucleophilic attack. Additional help origi-

nates in the enhanced nucleophilicity of the hydroxide group compared to the water molecule used in Figure 3. These concepts help to understand the origin of the catalytic proficiency of urease, which is discussed below. They are supported by recent ab initio calculations of the interaction of urea with cluster models of the urease active site.³⁴ The ab initio calculations showed that urea coordination involves hydrogen bonding between one amide group of urea and the Ni-bridging hydroxide and is also stabilized by a hydrogen bond interaction with a water molecule bonded to the second Ni center. These interactions, taken together, increase the electrophilicity of the carbon atom (Figure 12). The combined effects lower the activation energy to 23 kcal/mol, assuming the latter to be defined by the formation of the tetrahedral intermediate.³⁴ The additional acceleration of the reaction can be attributed to the coordination of key residues of the protein with the substrate urea. This fact reinforces the importance of the conformation of the mobile flap, which modulates the interactions between urea and the protein, which ultimately lowers the resonance stabilization of urea.

To estimate the catalytic proficiency of urease, we use the k_{cat}/K_m value reported by Karplus, Pearson, and Hausinger¹ (1.4×10^6 M⁻¹ s⁻¹ at 310.15 K) and our calculated value for k_{non} . We obtain a value of 5.6×10^{32} M⁻¹, which indicates that urease is far more efficient than any enzyme studied to date. Orotidine monophosphate decarboxylase is currently considered to be the most proficient enzyme known with $(k_{cat}/K_m)/k_{non} = 10^{22}$.¹⁴

Values close to 10^{16} have been reported for cytidine deaminase, AMP nucleosides, and adenosine deaminase, and a 10^{19} value has been reported for staphylococcal nuclease.¹⁴

The proficiency of an enzyme is related to the stability of the transition state structure involved in the catalytic mechanism. Because of the high binding energy of the TS, the most proficient enzymes are more sensitive to reversible inhibitors that are designed to resemble it. Knowledge of the characteristics of the TS provides a great deal of information to design specific inhibitors for the reaction type in which they are involved. For this reason, the mechanism associated with the catalytic decarboxylation of orotidine monophosphate has been extensively studied, both theoretically and experimentally.^{14–16,37–40} Our calculated value for urease proficiency suggests that this enzyme should be very sensitive to transition-state inhibitors.

Urease-inhibited systems have been analyzed, and the X-ray crystallographic structures have been reported.^{35,36,41–43} Difference maps showing tetrahedral pieces of electron densities in the vicinity of the Ni atoms have been identified in several cases and associated with a tetrahedral molecule that replaces the cluster of four water/hydroxide molecules found in the native enzyme.^{35,36} The structural characteristics of the inhibitors, which determine the H-bond coordination motif, are responsible for the conformation of the mobile flap, which orients key residues of the protein. Diamidophosphate (DAP) has been identified as a strong urease inhibitor.³⁵ Its tetrahedral coordination to the dinickel center keeps the flap closed and is believed to closely resemble the structure of the TS of the hydrolytic decomposition of urease. The overlap of I3a (Figure 3a) with DAP coordinated to urease from *Bacillus pasteurii* (PDB ID 3UBP)^{35,36,43} (Figure 14) shows that the optimized intermediate I3a can simultaneously coordinate both Ni centers of the urease 3UBP active site with one oxygen and one nitrogen atom. This coordination capability suggests that I3a is a good model of the tetrahedral intermediate generated in the urease-catalyzed hydrolysis of urea.

Conclusions

In this article, we report a comprehensive study of the mechanism of urea decomposition in solution phase, considering both elimination and hydrolytic pathways. In agreement with the available experimental evidence and supporting the fact that the uncatalyzed hydrolysis of urea has never been observed, we calculate a lower activation energy for the elimination mechanism. Water assists in lowering the activation barrier of the elimination reaction. The coordination of one water molecule affords the most energetically economic path, which proceeds through a six-member transition-state intermediate. A different coordination mode of a single water molecule triggers the

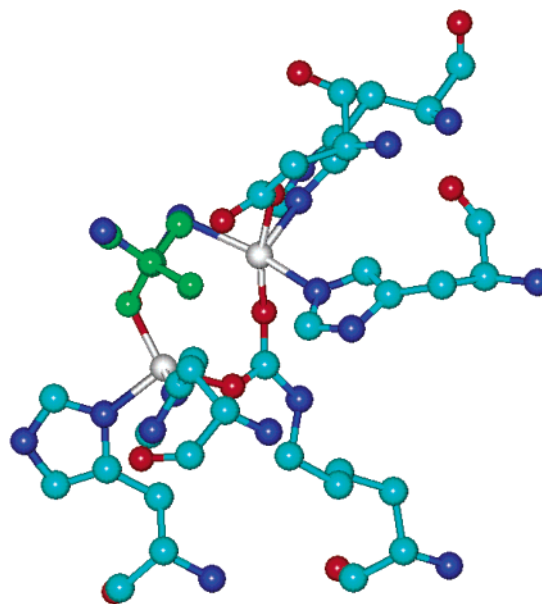


Figure 14. Superposition of I3a (from Figure 3a, in green) with the DAP moiety of 3UBP. Hydrogens not shown for clarity.

hydrolytic mechanism, and we postulate that this closely resembles what might occur in the active site of urease.

We have initially calculated the thermodynamic and kinetic parameters for the elimination mechanism, for which experimental data are available, attaining excellent agreement. On the basis of this accuracy, we have also calculated the kinetic parameters for the uncatalyzed hydrolysis, which have never been determined. The calculated kinetic parameters have allowed us to estimate the proficiency of urease. Using this information, we predict that urease is the most proficient enzyme identified to date.

Our calculations strongly support the enzymatic mechanism previously proposed that proceeds through a tetrahedral intermediate. They also help to understand the most significant features that contribute to the reduction of the activation energy in the enzyme active site. According to our model, polarization of the carbonyl group appears to be the key issue. Polarization is achieved through coordination of the urea protons to electron-withdrawing groups, which activate the carbon atom toward nucleophilic attack, which together with a hydroxide group results in a facile hydrolysis reaction. These concepts provide a molecular level explanation for the origin of the catalytic proficiency of urease.

Acknowledgment. G.E. is a member of the scientific career of the Argentine National Research Council (CONICET), Argentina. G.E. is on leave from DQAIHQ, Facultad de Ciencias Exactas y Naturales, Universidad de Buenos Aires, and Departamento de Química, Facultad de Ciencias Exactas, Universidad Nacional de La Plata, Argentina. We thank the National Center for Supercomputer Applications (NCSA) for generous allocations of supercomputer time. We thank the NIH via Grant GM066859 for generous support of this research.

Note Added after ASAP: References incorrectly numbered in 5/7/2004 version. Final version and print version are correct.

JA049327G

- (35) Musiani, F.; Arnofi, E.; Casadio, R.; Ciurli, S. *J. Biol. Inorg. Chem.* **2001**, *6*, 300.
 (36) Benini, S.; Rypniewski, W. R.; Wilson, K. S.; Ciurli, S.; Mangani, S. *J. Biol. Inorg. Chem.* **2001**, *6*, 778.
 (37) Lee, J. K.; Houk, K. N. *Science* **1997**, *276*, 942.
 (38) Beak, P.; Siegel, B. *J. Am. Chem. Soc.* **1976**, *98*, 3601.
 (39) Acheson, S. A.; Bell, J. B.; Jones, M. E.; Wolfenden, R. *Biochemistry* **1990**, *29*, 3198.
 (40) Shostak, K.; Jones, M. E. *Biochemistry* **1992**, *31*, 12155.
 (41) Benini, S.; Rypniewski, W. R.; Wilson, K. S.; Miletti, S.; Ciurli, S.; Mangani, S. *Struct. Fold. Des.* **1999**, *7*, 205.
 (42) Benini, S.; Rypniewski, W. R.; Wilson, K. S.; Ciurli, S.; Mangani, S. *J. Biol. Inorg. Chem.* **1998**, *3*, 268.
 (43) Benini, S.; Rypniewski, W. R.; Wilson, K. S.; Miletti, S.; Ciurli, S. *J. Biol. Inorg. Chem.* **2000**, *5*, 110.